3-23-2023

Analytical Method for Predicting Lateral Facing Deflection of Geosynthetic-Reinforced Soil Abutment Walls

Thang Pham

S. Mustapha Rahmaninezhad

Andres Palma

Truc Phan

Thuy Vu

Analytical Method for Predicting Lateral Facing Deflection of Geosynthetic-Reinforced Soil Abutment Walls

Thang Pham, Ph.D., P.E., A.M.ASCE[1,*], S. Mustapha Rahmaninezhad, Ph.D., A.M.ASCE[2], Andres Palma, P.E.[3], Truc Phan[4], and Thuy Vu, Ph.D.[5]

[1]Assistant Professor, Civil Engineering Dept., University of Texas Rio Grande Valley, Edinburg, TX (*Corresponding Author). E-mail: thang.pham@utrgv.edu
[2]Assistant Professor of Practice, Civil Engineering Dept., University of Texas Rio Grande Valley, Edinburg, TX. Email: m.rahmaninezhad@utrgv.edu
[3]Engineering Manager, Millennium Engineers Group Inc., Pharr, TX. E-mail: apalma@megengineers.com
[4]Ph.D. Student, Dept. of Civil Engineering, National Taipei University of Technology, Taiwan, Email: phantranthanhtruc@muce.edu.vn
[5]Associate Professor, Civil Engineering Dept., University of Texas Rio Grande Valley, Edinburg, TX. Email: thuy.vu@utrgv.edu

ABSTRACT

Geosynthetic-reinforced soil (GRS) walls have been recently used as bridge abutments to directly support spread footings on the reinforced soil mass. This application reduces the requirement for using traditional deep foundations, such as piles or drilled shafts, to support bridge beams. GRS abutment walls are generally subjected to high footing loads that are close to the wall facing. Although GRS abutment walls with modular block facing have been the subject of a number of studies, there are limited methods to predict the profile of the lateral facing deflections along the height of the GRS abutment walls. Lateral deflections along the facing of GRS walls are of significant importance and are difficult to predict. In practice, design engineers need numerical modeling or software to predict the deflection profile. The objectives of this study were to develop an analytical approach to estimate lateral deflections of the wall facing along the height of the GRS abutment walls. Two sets of equations were developed, and experimental test results were used for verification of the proposed analytical approach. There is agreement between the results from proposed approach and the measured data. The maximum lateral deflections predicted from the proposed equations are almost identical to the measured data. The facing lateral deflection profiles with depth are within close range of measured data. The proposed analytical equations for determining lateral deflections provide an effective and simple tool in design of the GRS abutment walls.

Keywords: Bridge Abutment; Lateral Deflection; GRS Wall; Block Facing

INTRODUCTION

Geosynthetic-reinforced soil (GRS) walls have been extensively used in transportation systems to retain and support backfill soil, roadways and railways, bridges, and traffic loads (Berg et al. 2009, Wu et al. 2013, Wu and Pham 2013, Tatsuoka et al. 2014, Han 2021). In recent years, GRS walls have been also employed as bridge abutments to directly support spread footings (Helwany et al. 2003, Lee and Wu 2004, Wu et al. 2006, Kakrasul et al. 2018, Xie et al. 2019, Rahmaninezhad et

al. 2020). This technology has been successfully utilized instead of using traditional deep foundations (such as piles and shafts) within GRS walls. Fig. 1 illustrates a typical cross-section of a GRS wall-supported footing with a modular block facing as a bridge abutment (GRS abutment wall). The considerable advantage of this technology is to minimize bumps at the end of bridges as compared with using traditional deep foundations (Skinner and Rowe 2005, Rahmaninezhad 2019). Bumps at the end of bridges often occur due to the differential settlement between pile-supported abutments and approaching structures (Rahmaninezhad 2019 and 2021).

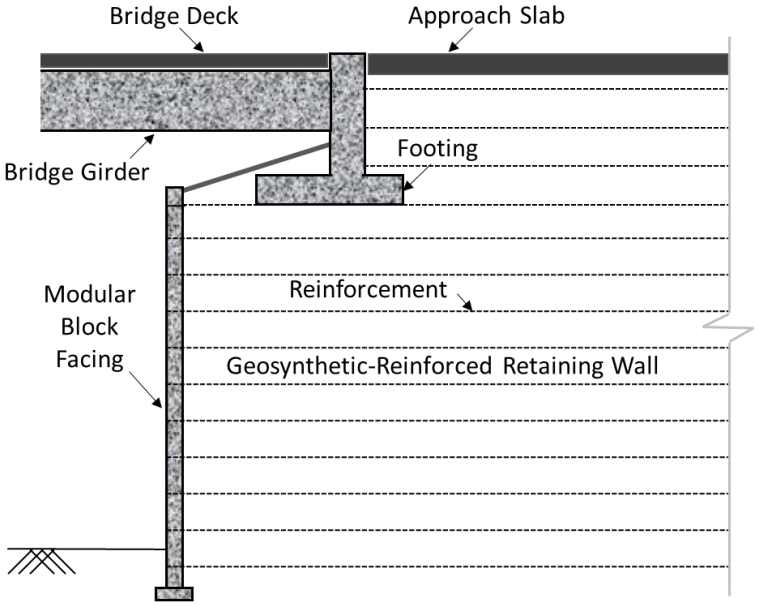

Figure 1. Typical cross-section of a GRS wall-supported footing as bridge abutment (GRS abutment wall).

As shown in Figure 1, different from conventional GRS walls, the GRS abutment walls are generally subjected to high footing loads. To reduce bridge spans, the footings are often placed close to the facing of the GRS walls. Therefore, the footing loads induce additional lateral deflections on the flexible facing of GRS walls. Although several methods are available to estimate the lateral deflections of conventional GRS walls without footing loading (i.e., Jewell and Milligan 1989, Giroud 1989, Christopher et al. 1990, Wu 1994, Pham 2009, Krystyna et al. 2021), so far, there are limited methods available to predict the lateral deflection for the GRS abutment walls with flexible facing.

Abu-Hejleh et al. monitored the facing deflection and strain in geogrid reinforcements of GRS abutment walls during construction and under service loads. Abu-Hejleh et al. found that the maximum lateral deflection of the facing occurred within the upper third of all walls of different heights. Abu-Hejleh et al. also found that the calculated lateral deflection using the measured strain in the reinforcements had a good agreement with the measured lateral facing deflection. The Federal Highway Administration (FHWA 2012) method for the geosynthetic-reinforced soil integrated bridge system (GRS-IBS) suggested a method using the vertical settlement of the footings to calculate the maximum lateral deflection for the GRS abutment walls. The GRS-IBS wall is a special application of the GRS wall as the bridge abutment with bridge girders directly placed on the top of the wall. In the FHWA method for the GRS-IBS walls, conservatively, a zero-volume change within a GRS abutment wall was assumed by Adams et al. (2012) to predict the

lateral facing deflection of the abutment wall. Moreover, the FHWA suggested the maximum lateral deflection of the facing (induced by footing loads) should be less than one percent (1%) of the footing width and the setback distance of the footing to the front of the wall facing. However, Saghebfar et al. found a significant difference between the predicted lateral facing deflection of the wall using the FHWA method for the GRS-IBS walls and the measured lateral deflections in the field.

Xiao et al. (2016) carried out a series of model tests on the GRS abutment walls to evaluate the effects of the setback distance, the footing width, and the length of geogrid reinforcement on the lateral facing deflection of the GRS abutment walls. Xiao et al. (2016) found that when the setback distance was small, the location of maximum lateral deflection in facings with mechanical connection was within the upper portion of the wall facing. Zheng et al. (2019) studied the static response of four half-scale GRS abutment walls modular block facing. Zheng et al. (2019) evaluated the effects of footing pressure, vertical spacing, and geogrid tensile stiffness on the lateral facing deflection of the abutment walls. They reported the measured lateral deflection increased with elevation along with the facing, higher footing pressure, reduced geogrid tensile stiffness, and larger vertical spacing.

Khosrojerdi et al. (2020) developed a method based on a numerical parametric study to predict the maximum lateral deflection of GRS abutment walls induced by footing loading. The parameters that are considered by Khosrojerdi et al. (2020) in their prediction method include wall height, facing's batter, foundation width, backfill friction angle, reinforcement stiffness, vertical spacing, reinforcement length, and applied load. The proposed method by Khosrojerdi et al. (2020) does not consider the effects of the setback distance on the maximum lateral deflection, while Xiao et al. (2016) found that the lateral deflection in the walls with smaller setback distances was larger than the walls with larger setback distances. Rahmaninezhad and Han (2021) investigated the effect of footing loading on the stability of 68 GRS abutment walls with flexible facing (wrap-around and modular block facing). Rahmaninezhad and Han (2021) utilized the limit equilibrium method (i.e., the modified Bishop method) to determine factors of safety of these abutment walls. Then, Rahmaninezhad and Han (2021) carried out data analysis and developed a relationship between the maximum lateral facing deflection and the factor of safety of the GRS abutment walls with flexible facing.

DEVELOPING ANALYTICAL EQUATIONS FOR LATERAL DEFLECTION OF GRS WALLS

For retaining walls that have wrapped facing or facing with neglectable rigidity, Jewell and Milligan (1989) developed design charts to estimate wall facing lateral deflection when walls subject to uniform load. In this method, the reinforcement length to wall height ratio, L/H, is equal to 0.7. The ideal length of 0.7H is commonly used in practice. Rowe and Ho (1998) based on a series of numerical analyses of GRS walls showed that the maximum lateral deflection obtained by the Jewell-Milligan method is generally in good agreement with the numerical results for L/H of 0.7.

In this study, the developed method by Jewell and Milligan (1989) for calculating the lateral deflection along the height of GRS walls with wrap facing were modified to include the effects of footing loads in GRS abutment walls with modular block facing.

1. Lateral Deflection of Reinforced Soil Walls with Wrapped Facing

Figure 2 shows the three major zones in a GRS wall and the force distribution in the reinforcement at depth z_i, used by Jewell and Milligan (1989) to develop an analytical model for determination of wall deflection. Jewell and Milligan (1989), without giving the derivation, have presented design charts based on the analytical model. The following derivation is presented for completeness and for easier reference when presenting the derivation of the analytical model developed in this study. It is assumed that the tensile strain of the geosynthetic reinforcement is equal to the wall lateral deflection at the reinforcement depth, and the load is applied uniformly throughout the surface. When there is a large footing in Active Zone 1 (Figure 2), the footing load alters the load distribution on the facing and geosynthetic layers, and reinforcement tensile force is affected, and will be discussed in the next section.

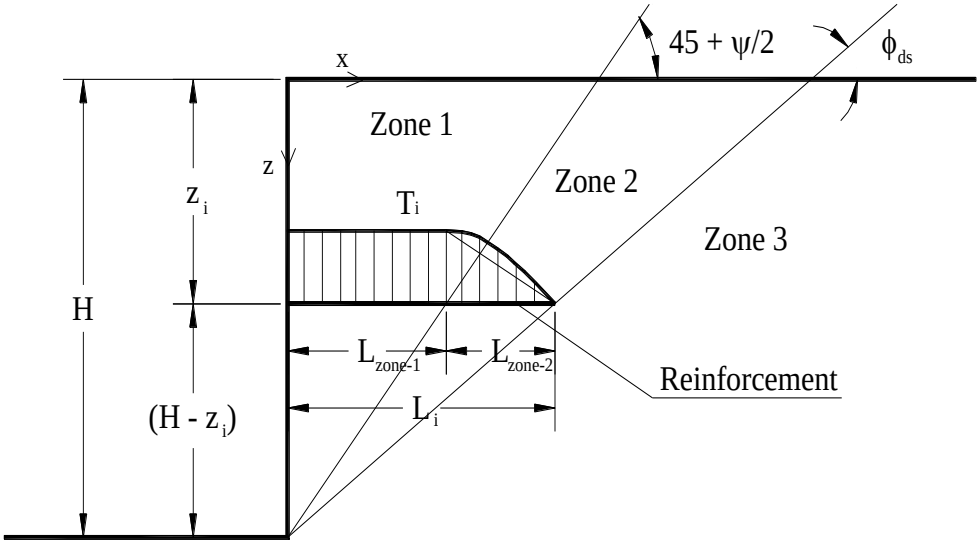

Figure 2. Major zones of the reinforcement force in a reinforced soil wall (Jewell and Milligan, 1989).

Lateral deflection, Δ_h, of the wall face at depth z_i can be evaluated as:

$$\Delta_h = \Delta_{zone\text{–}1} + \Delta_{zone\text{–}2} \tag{1}$$

$$\Delta_{zone\text{–}1} = \int_0^{L_{zone\text{-}1}} \frac{T_i}{K_{reinf}}\, dx = \frac{T_i}{K_{reinf}} L_{zone\text{–}1} \tag{2}$$

$$\Delta_{zone\text{–}2} = \int_{L_{zone\text{-}1}}^{L_{zone\text{-}1}+L_{zone\text{-}2}} \frac{T}{K_{reinf}}\, dx \approx \left(\frac{1}{2}\right) \frac{T_i}{K_{reinf}} L_{zone\text{–}2} \tag{3}$$

where K_{reinf} is stiffness of the reinforcement, T is reinforcement force at depth z_i in Zone 2, T_i is the connection force or the maximum reinforcement force at depth z_i, $L_{zone\text{-}1}$ is reinforcement length in Zone 1 at depth z_i, and $L_{zone\text{-}2}$ is reinforcement length in Zone 2 at depth z_i; H is wall height; ϕ_{ds} is the effective direct shear friction angle of soil; ψ is the angle of dilation of the backfill material. Substituting Eqs. 2 and 3 into Eq. 1 then

$$\Delta_h = \frac{T_i}{K_{reinf}} \left(L_{zone\text{–}1} + \frac{1}{2} L_{zone\text{–}2} \right) \tag{4}$$

Since

$$L_{zone-1} = (H - z_i)\tan\left(45^o - \frac{\psi}{2}\right) \quad (5)$$

and

$$L_{zone-2} = (H - z_i)\left[\tan(90^o - \phi_{ds}) - \tan\left(45^o - \frac{\psi}{2}\right)\right] \quad (6)$$

then substituting Eqs. 5 and 6 into Eq. 4 leads to

$$\Delta_h = \frac{T_i}{K_{reinf}}\left\{(H - z_i)\tan\left(45^o - \frac{\psi}{2}\right) + \frac{1}{2}(H - z_i)\left[\tan(90^o - \phi_{ds}) - \tan\left(45^o - \frac{\psi}{2}\right)\right]\right\} \quad (7)$$

Rearranging Eq. 7, then

$$\Delta_h = \frac{T_i}{K_{reinf}}(H - z_i)\left\{\tan\left(45^o - \frac{\psi}{2}\right) + \frac{1}{2}\left[\tan(90^o - \phi_{ds}) - \tan\left(45^o - \frac{\psi}{2}\right)\right]\right\} \quad (8)$$

or

$$\Delta_h = \frac{T_i}{K_{reinf}}(H - z_i)\left\{\frac{1}{2}\left[\tan\left(45^o - \frac{\psi}{2}\right) + \tan(90^o - \phi_{ds})\right]\right\} \quad (9)$$

The value of lateral defection, Δ_h, of a GRS wall at depth z_i, can be calculated directly from the following equation:

$$\Delta_h = \left(\frac{1}{2}\right)\left(\frac{T_i}{K_{reinf}}\right)(H - z_i)\left[\tan\left(45^0 - \frac{\psi}{2}\right) + \tan(90^0 - \phi_{ds})\right] \quad (10)$$

2. Connection Forces for GRS Walls with Modular Block Facing

Forces acting on two adjacent facing blocks at depth z_i are sketched in Figure 3. The tensile connection force in the reinforcement at depth z_i can be expressed as:

$$T_i = K_a(\gamma_s z_i + q)S_v - \gamma_b b S_v \tan\delta\,(1 + \tan\delta\tan\beta) \quad (11)$$

where K_a is active earth pressure coefficient; γ_s is unit weight of the backfill; γ_b is unit weight of facing block; b is width of facing block; S_v is reinforcement spacing; δ is friction angle between modular block facing elements (δ can be the friction angle between facing blocks if there is no reinforcement between the blocks, or it can be the friction angle between facing block and geosynthetic if there is reinforcement sandwiched between blocks); β is friction angle between back face of wall and soil. Note that if the friction between the back face of the wall facing and the soil behind the wall is ignored, the connection force at depth z_i becomes:

$$T_i = K_a(\gamma_s z_i + q)S_v - (\gamma_b b S_v)(\tan\delta) \quad (12)$$

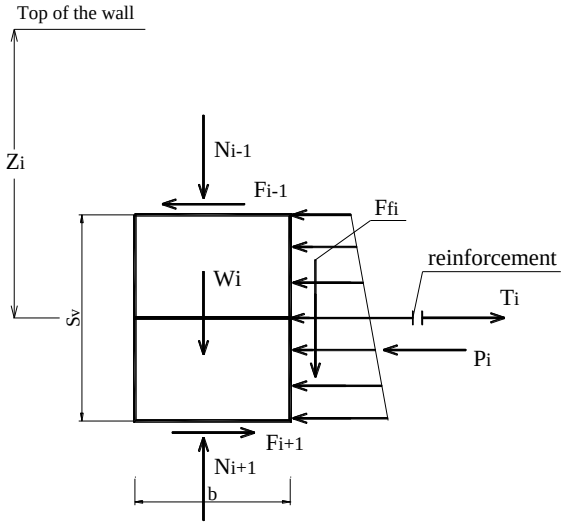

Figure 3. Forces acting on two adjacent facing blocks at depth z_i.

3. Predicting Lateral Deflection of Reinforced Soil Walls with Modular Block Facing

From Eqs. 10 and 11, the deflection of a GRS wall with modular block facing at depth z_i can be determined by:

$$\Delta_i = \frac{K_a(\gamma_s z_i + q)S_v - \gamma_b b S_v \tan\delta(1+\tan\delta\tan\beta)}{2K_{reinf}}(H - z_i)\left[\tan\left(45^0 - \frac{\psi}{2}\right) + \tan(90^0 - \varphi_{ds})\right] \quad (13)$$

Eq. 13 is referred to as *the analytical model* for GRS walls. When the friction between the soil and the back face of the wall facing is insignificant, Eq.13 becomes:

$$\Delta_i = 0.5\left(\frac{K_a(\gamma_s z_i + q)S_v - (\gamma_b b S_v)(\tan\delta)}{K_{reinf}}(H - z_i)\left[\tan\left(45^0 - \frac{\psi}{2}\right) + \tan(90^0 - \varphi_{ds})\right]\right) \quad (14)$$

Note that the lateral deflections calculated from Eq. 14 are slightly greater than those calculated by Eq. 13.

DEVELOPING ANALYTICAL EQUATIONS FOR LATERAL DEFLECTION OF REIFORCED SOIL BRIDGE ABUTMENTS

In this study, the proposed approach for predicting the lateral deflection along the height of GRS walls with wrap facing and modular block facing was developed to include the effects of footing loads in GRS abutment walls. Figure 4(a) shows the typical cross section of a GRS bridge abutment. The development of the approach is as follows.

1. Predicting Vertical Stress with Depth

Based on the current design methods, the vertical stress of the soil under the bridge footing can be calculated using Rankine formula as recommended from FHWA (2009), as in Figure 4. For strip footing, the vertical increased stress (induced stress) can be calculated using the simplified equations below.

At depth $z \le z_1$, there is no increased stress due to the footing load acting on facing, and the increased vertical stress right under the footing is

$$\Delta\sigma_v = \frac{Q_v}{D_1} = \frac{Q_v}{b_f + z} \quad (15)$$

and at depth $z > z_1$,

$$\Delta\sigma_v = \frac{Q_v}{D_1} = \frac{Q_v}{\frac{b_f + z}{2} + d} \tag{16}$$

where z is the depth from the base of the bridge footing; Q_v is the linear applied load of strip footing (kN/m); b_f is the width of applied load or equivalent footing width by reducing it by $2e'$, where e' is the eccentricity of the footing b_f minus $2e'$; d is the distance from the facing to the center of the footing; D_1 is the effective width of applied load at any depth; z_1 is the depth where the effective width intersects back of the wall face z_1 is equal to $2d$ minus b_f.

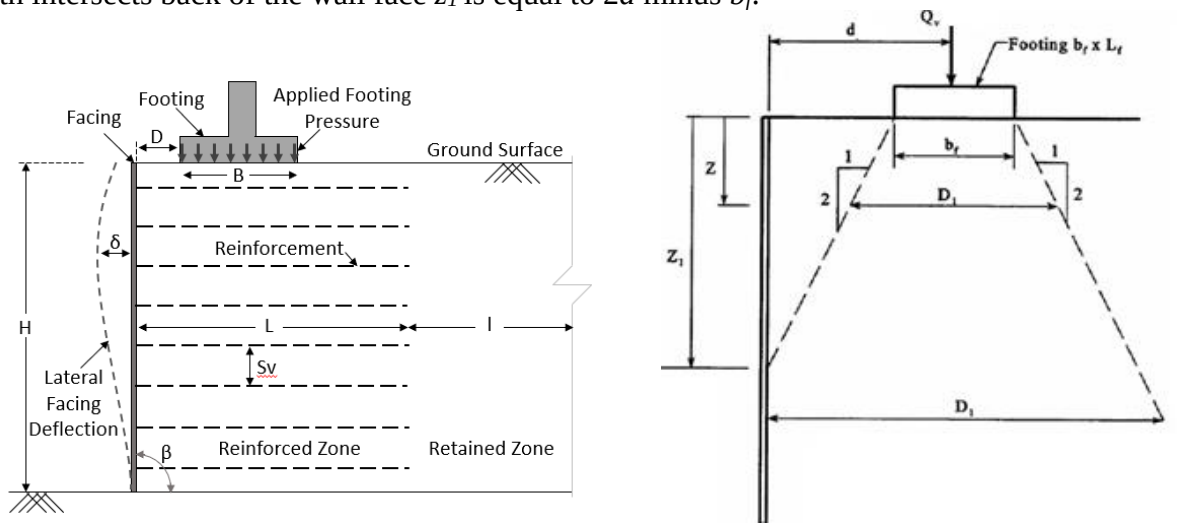

(a) **(b)**

Figure 4. (a) Typical cross-section of a GRS wall to support a spread footing (b) Vertical induced stress distribution, FHWA (1990)

2. Predicting Lateral Stress with Depth

Lateral stress (σ_h) acting near the wall facing can be determined:

At depth $z \leq z_1$, $\sigma_h = K_a\sigma_v = K_a(\gamma z + \Delta\sigma_v) = K_a(\gamma z)$ (17)

At depth $z > z_1$, $\sigma_h = K_a\sigma_v = K_a(\gamma z + \Delta\sigma_v) = K_a\left(\gamma z + \frac{Q_v}{\frac{b_f + z}{2} + d}\right)$ (18)

For wrapped face at the active zone near the facing zone, the tension connection force T_i (kN/m) at each layer of reinforcement is calculated using the following equation:

$$T_i = \sigma_h S_v \tag{19}$$

The term S_v is equal to the vertical reinforcement spacing for a layer where vertically adjacent reinforcements are equally spaced from the layer under consideration, and lateral earth pressure σ_h is calculated at the depth z of the reinforcement.

3. Predicting Lateral Deflection of GRS Bridge Walls with Negligible Facing Rigidity (wrapped face)

The value of lateral deflection Δh at depth z_i of a GRS wall with uniform loads throughout the surface, can be calculated directly from Eq. 10. For bridge abutment walls, the strip loads from the footing should be included into Eq. 10. As noted by Jewell and Milligan (1989), in active Zone 1, the principal stresses are not rotated. However, the spread footing load causes principal stress rotations when depth $z \leq z_1$, hence Eq. 10 needs modifications.

At depth $z \leq z_1$, the length of reinforcement in Zones 1 and 2 are modified as:

$$L_{Zone-1} = (H - z_1)tan(26.6^o) \quad (20)$$

and

$$L_{Zone-2} = (H - z_1)[tan(90^o + \emptyset_{ds}) - tan(26.6^o)]. \quad (21)$$

Substituting Eqs. 5 and 6 into Eq. 4 leads to

$$\Delta_h = \frac{T_i}{K_{reinf}}\left\{(H - z_1)tan(26.6^o) + \frac{1}{2}(H - z_1)[tan(90^o + \emptyset_{ds}) - tan(26.6^o)]\right\} \quad (22)$$

Rearrange Eq. 22, then

$$\Delta_h = \frac{T_i}{K_{reinf}}(H - z_1)\left\{tan(26.6^o) + \frac{1}{2}[tan(90^o + \emptyset_{ds}) - tan(26.6^o)]\right\} \quad (23)$$

or

$$\Delta_h = \left(\frac{1}{2}\right)\left(\frac{T_i}{K_{reinf}}\right)(H - z_1)[tan(26.6^o) + tan(90^o + \emptyset_{ds})] \quad (24)$$

T_i can be calculated from Eqs. 17 and 19, therefore, substituting these two into Eq. 24 yields

$$\Delta_h = (0.5)\left(\frac{K_a(\gamma z)S_v}{K_{reinf}}\right)(H - z_i)[tan(26.6^o) + tan(90^o + \emptyset_{ds})] \quad (25)$$

At depth $z > z_1$, substituting Eqs. 18 and 19 into Eq.10 into obtain:

$$\Delta_h = (0.5)\left(\frac{K_a\left(\gamma z + \frac{Q_v}{\frac{b_f + z}{2} + d}\right)S_v}{K_{reinf}}\right)(H - z_i)\left[tan\left(45^0 - \frac{\psi}{2}\right) + tan(90^0 - \emptyset_{ds})\right] \quad (26)$$

or,

$$\Delta_h = S_v K_a\left(\frac{H - z_i}{2K_{reinf}}\right)\left(\gamma z + \frac{Q_v}{\frac{b_f + z}{2} + d}\right)\left[tan\left(45^0 - \frac{\psi}{2}\right) + tan(90^0 - \emptyset_{ds})\right] \quad (27)$$

Eqs. 20 and 22 can be used for calculating profile of the lateral facing deflections along with the height of wrapped facing wall (or negligible facing rigidity) of GRS bridge abutment.

4. Predicting Lateral Deflection of GRS Bridge Walls with Modular Block Facing

For the case with modular block facing, equations were also developed to predict lateral deflection of GRS bridge walls. At depth $z \le z_1$, substituting Eqs. 17 and 19 into modified Eq. 13 with the reinforcement length for zones 1 and 2 using Eqs. 20 and 21 to obtain:

$$\Delta_i = 0.5\,\frac{K_a(\gamma z)\,S_v - \gamma_b b S_v \tan\delta(1+\tan\delta\tan\beta)}{K_{reinf}}(H - z_i)\left[tan(26.6^o) + tan(90^o + \emptyset_{ds})\right] \quad (28)$$

or,

$$\Delta_i = \frac{(H - z_i)}{2K_{reinf}}[K_a\gamma z\,S_v - \gamma_b b S_v\,tan\,\delta\,(1 + tan\,\delta\,tan\,\beta)]\left[tan(26.6^o) + tan(90^o + \emptyset_{ds})\right] \quad (29)$$

At depth $z > z_1$, substituting Eqs. 18 and 19 into Eq. 14 to obtain:

$$\Delta_i = 0.5\,\frac{K_a\left(\gamma z + \frac{Q_v}{\frac{b_f + z}{2} + d}\right) - \gamma_b b S_v \tan\delta(1+\tan\delta\tan\beta)}{K_{reinf}}(H - z_i)\left[\tan\left(45^0 - \frac{\psi}{2}\right) + \tan(90^0 - \varphi_{ds})\right] \quad (30)$$

or,

$$\Delta_i = \frac{(H-z_i)}{2K_{reinf}} \left[K_a \left(\gamma z + \frac{Q_v}{\frac{b_f+z}{2}+d} \right) - \gamma_b b S_v \tan\delta \, (1 + \tan\delta \tan\beta) \right] \left[\tan\left(45^0 - \frac{\psi}{2}\right) + \tan(90^0 - \varphi_{ds}) \right] \quad (31)$$

Eqs. 29 and 31 are referred to as *the analytical equations*, and they can be used for predicting profile of lateral facing deflection along modular block facing of GRS bridge abutment walls.

VERIFICATION OF THE PROPOSED ANALYTICAL EQUATIONS

Eqs. 10 and 13 are for predicting lateral deflection of GRS walls with wrapped facing and modular block facing; and Eqs. 29 and 31 are for predicting lateral defections of GRS bridge abutments with modular block facing. The two sets were developed based on the same principles. In this study, Eq. 13 (and therefore Eq. 14) was verified using measured data from large-scale experiments. Figure 5 shows the configuration a large-scale experiment of GRS wall with modular block facing "Wall 1" of a series of laboratory experiments conducted by Hatami and Bathurst (2006). The parameters of the wall are summarized below: Wall: height H of 3.6 m with a facing batter of 8° from the vertical; Soil: a clean uniform beach sand, γ_s of 16.8 kN/m^3, ϕ_{ps} of 44^o, ψ of 11^o, and c of 2 kPa; Geosynthetic reinforcement: a weak biaxial polypropylene (PP) geogrid, vertical spacing of 0.6 m, reinforcement stiffness of 115 kN/m, ultimate strength of 14 kN/m; Facing: solid masonry concrete blocks (300 mm wide by 150 mm high by 200 mm deep), and γ_b of 20 kN/m^3; Interface between facing blocks: $\delta_{b\text{-}b}$ of 57^o and $c_{b\text{-}b}$ of 46 kPa.

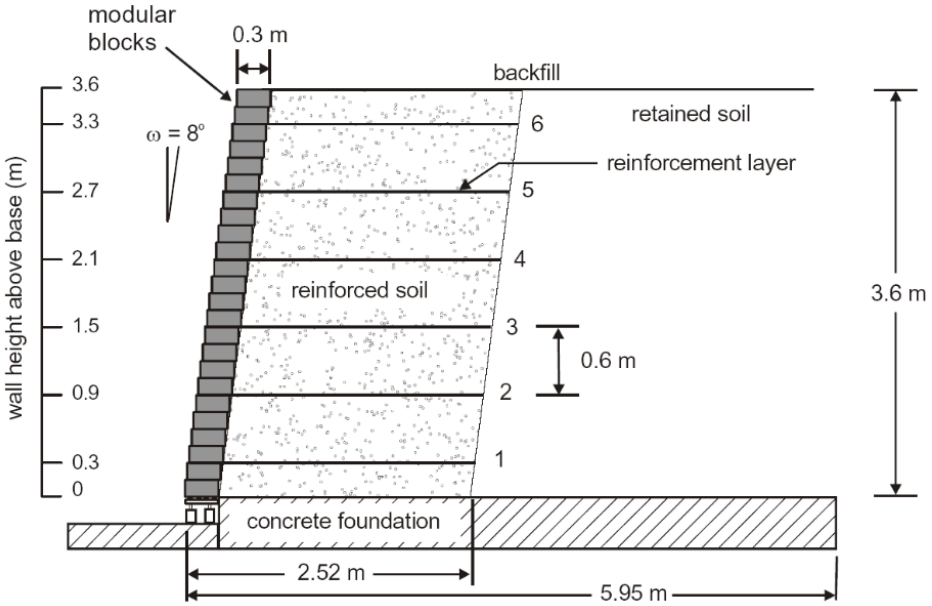

Figure 5. Configuration of a large-scale experiment of GRS wall with modular block facing (Hatami and Bathurst, 2006).

Because the analytical model requires that the direct shear friction angle be used in model calculations, and it also assumes a vertical wall face, the direct shear friction angle of the soil and the facing batter factor were determined before using the analytical model to evaluate the lateral deflection of the facing.

Direct shear friction angle can be calculated as:

$$\tan \phi_{ds} = \frac{\sin \phi_{ps} \cos \psi}{1 - \sin \phi_{ps} \sin \psi} = \frac{\sin 44^o \cos 11^o}{1 - \sin 44^o \sin 11^o} = 40^o \quad (32)$$

The empirical facing batter factor, Φ_{fb}, from Allen and Bathurst (2001), with facing batter of 8°:

$$\Phi_{fb} = \left(\frac{K_{abh}}{K_{avh}} \right)^d = 0.88 \quad (33)$$

where K_{abh} is the horizontal component of the active earth pressure coefficient accounting for wall face batter, K_{avh} is the horizontal component of the active earth pressure coefficient for a vertical wall, and d is a constant coefficient. Allen and Bathurst (2001) found that the value of d of 0.5 would yield the best fit for available T_{max} data, and this value is recommended for determination of Φ_{fb}.

Figure 6 shows lateral deflections of the wall under surcharge pressures of 50 kPa and 70 kPa. The figure shows the range of the measured minimum, mean, and maximum deflections from three sources: experiments (Hatami and Bathurst, 2006), calculated using Jewell-Milligan method, and calculated using the proposed analytical model. Lateral deflections calculated by the proposed analytical model are in good agreement with the average measured deflections from experiments, for both cases of surcharge pressures. Note that lateral deflections obtained from Jewell-Milligan method are as 3.5 times greater as the average measured deflections. One of the major contributions for the discrepancy is that Jewell-Milligan method does not consider the stiffness of the facing.

The maximum lateral deflections predicted from the proposed equations are almost identical to the measured results. The facing lateral deflection profiles with depth were created, and they are within the close range of measured data. The proposed Eq. 10 was developed based on Jewell-Milligan method, therefore, it can be used in place of the Jewell-Milligan's charts and it is easier to use. For lateral deflection of the bridge abutment, Eqs. 10 and 13 were modified to accommodate the footing loads. Two sets of equations used for predicting lateral deflections of the bridge abutments, Eqs. 29 and 31 are for walls with modular block facing, and Eqs. 25 and 27 are for walls without modular block facing. These equations can also be used for walls with applied loads, or for bridge abutments. Calculations of retaining wall deflections are complicated, usually require numerical modeling or software; these analytical equations help the analysis and design to be more convenient and cost effective.

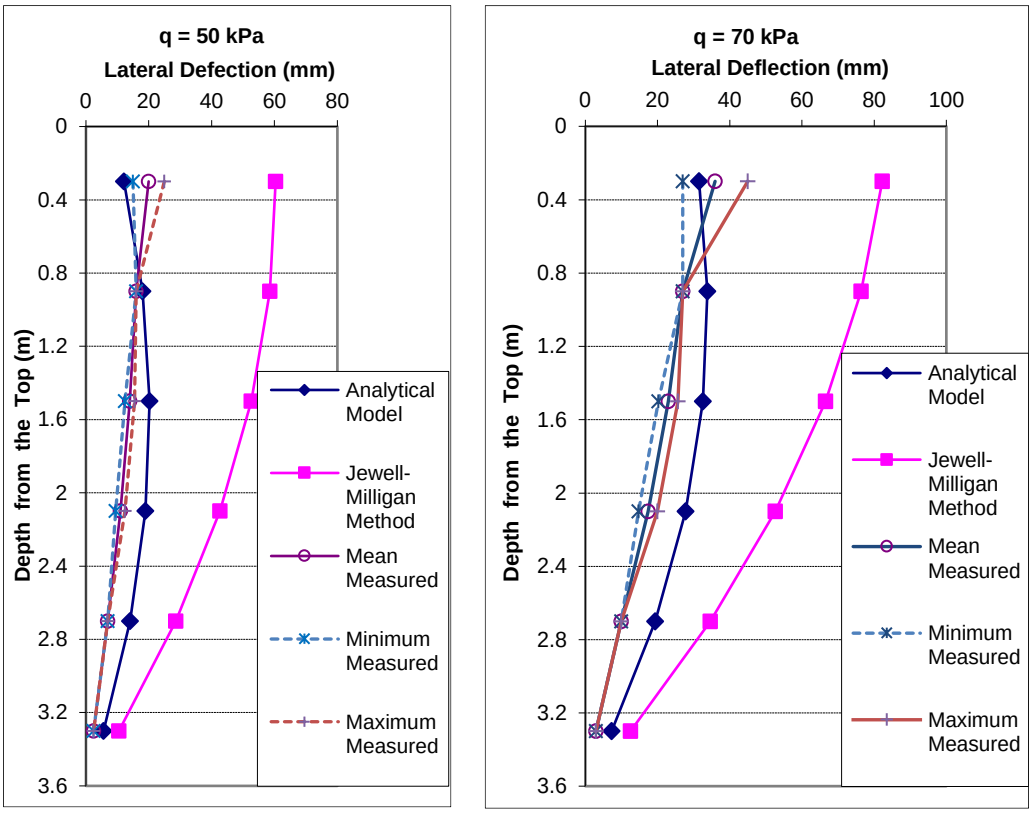

Figure 6. Comparison of measured lateral deflections from Jewell-Milligan method and the proposed approach.

CONCLUSION

Two sets of analytical equations were developed to predict lateral deflection profile of GRS walls and GRS bridge abutments with modular block facing. The analytical equations were verified using data from a large-scale experiment of GRS walls with modular block facing, and were compared with Jewell-Milligan method. The maximum lateral deflections predicted from the proposed equations are almost identical to the measured data. The facing lateral deflection profiles with depth are within a close range of measured data. The proposed analytical equations provide a simple and improved approach for predicting lateral deflections with depth of a GRS wall with modular block facing and GRS bridge abutments. Calculations of retaining wall deflections usually require numerical modeling or software; these analytical equations help the analysis and design to be more convenient and cost effective.

REFERENCES

Adams, M., Nicks, J., Stabile, T., Schlatter, W. and Hartmann, J. (2012). *Geosynthetic reinforced soil integrated bridge system, interim implementation guide (No. FHWA-HRT-11-026).* Federal Highway Administration.

Berg, R.R., Christopher, B.R. and Samtani, N.C. (2009). *Design and construction of mechanically stabilized earth walls and reinforced soil slopes. US Department of Transportation*, Federal Highway Administration.

Christopher, B.R., Gill, S.A., Giroud, J.P., Juran, I., Mitchell, J.K., Schiosser, F. and Dunnicliff, J. (1990). *Reinforced Soil Structures, Vol. I: Design and Construction Guidelines. Report No. FHWA-RD-89-043.* Federal Highway Administration.

Giroud, J.P. (1989). *Geotextile engineering workshop-design examples. Rep. No. FHWA-HI-89, 2*. Federal Highway Administration.

Han, J. (2021). "Limit equilibrium analysis and design of geosynthetic-reinforced fill walls under special conditions." *Indian Geotechnical Journal*, 51(1), pp.50-62.

Hatami K. and Bathurst R. J. (2006). "Numerical Model for Reinforced Soil Segmental Walls under Surcharge Loading." *Journal of Geotechnical and Geoenvironmental Engineering*, ASCE, 132(6), 673-684.

Helwany, S.M., Wu, J.T., Froessl, B. (2003). "GRS bridge abutments—an effective means to alleviate bridge approach settlement." *Geotextiles and Geomembranes*, 21(3), pp. 177-196.

Jewell, R. A., and Milligan, G. W. E. (1989). "Deformation calculation for reinforced soil walls." *Proc., 12th International Conference on Soil Mechanics and Foundation Engineering,* Vol. 2. Taylor & Francis, Abingdon, U.K., pp. 1259–1262.

Krystyna Kazimierowicz-Frankowska, Marek Kulczykowski (2021). "Deformation of model reinforced soil structures: Comparison of theoretical and experimental results." *Geotextiles and Geomembranes*, Volume 49, Issue 5, pp. 1176-1191.

Khosrojerdi, M., Xiao, M., Qiu, T. and Nicks, J. (2020). "Prediction equations for estimating maximum lateral displacement and settlement of geosynthetic reinforced soil abutments." *Computers and Geotechnics,* 125, p.103622.

Kakrasul, J.I., Han, J., and Rahmaninezhad, S.M. (2018). "Laboratory evaluation of deformations of geosynthetic-reinforced retaining walls subjected to footing loading." *11th International Conference on Geosynthetics,* Seoul, Korea.

Lee, K.Z., Wu, J.T. (2004). "A synthesis of case histories on GRS bridge-supporting structures with flexible facing." *Geotextiles and geomembranes,* 22 (4), pp. 181-204.

Pham Q. T. (2009). "Investigating Composite behavior of Geosynthetic-Reinforced Soil (GRS) Mass." *Ph.D. Dissertation,* University of Colorado Denver.

Rahmaninezhad, S.M., Han, J. (2021). "Lateral facing deflections of geosynthetic-reinforced retaining walls under footing loading." *Transportation Geotechnics,* 30 (2021) 100594

Rahmaninezhad, S.M., Han, J., Al-Naddaf, M., and Mamaghanian, J. (2021). "Limit equilibrium analysis of geosynthetic-reinforced retaining wall-supported footings." *2021 Geosynthetics Conference Proceedings,* pp. 691-701.

Rahmaninezhad, S.M., Han, J. and Al-Naddaf, M. (2020). "Limit equilibrium analysis of geosynthetic-reinforced retaining walls subjected to footing loading." *In Geo-Congress 2020: Engineering, Monitoring, and Management of Geotechnical Infrastructure,* pp. 464-471.

Rahmaninezhad, S.M. (2019). "Geosynthetic Reinforced Retaining Walls with Flexible Facing under Footing Loading." *Ph.D. Dissertation,* Civil, Environmental and Architectural Engineering Department, The University of Kansas. Lawrence, KS, USA.

Saghebfar, M., Abu-Farsakh, M., Ardah, A., Chen, Q. and Fernandez, B.A. (2017). "Performance monitoring of geosynthetic reinforced soil integrated bridge system (GRS-IBS) in Louisiana." *Geotextiles and Geomembranes,* 45(2), pp. 34-47.

Skinner, G.D., Rowe, R.K. (2005). "Design and behaviour of a geosynthetic reinforced retaining wall and bridge abutment on a yielding foundation." *Geotextiles and geomembranes,* 23(3), pp. 234-260.

Tatsuoka, F., Tateyama, M., Koseki, J., Yonezawa, T. (2014). "Geosynthetic-reinforced soil structures for railways in Japan." *Transportation Infrastructure Geotechnology,* 1 (1), pp. 3-53.

Wu, J.T., Pham, T.Q. and Adams, M.T. (2013). *Composite behavior of geosynthetic reinforced soil mass (No. FHWA-HRT-10-077).* Federal Highway Administration.

Wu, J.T. and Pham, T.Q. (2013). "Load-carrying capacity and required reinforcement strength of closely spaced soil-geosynthetic composites." *Journal of Geotechnical and Geoenvironmental Engineering,* 139(9), pp.1468-1476.

Wu, J.T. (1994). *Design and construction of low cost retaining walls: The next generation in technology.* Colorado Transportation Institute.

Wu, J.T., Lee, K.Z. and Pham, T. (2006). "Allowable bearing pressures of bridge sills on GRS abutments with flexible facing." *Journal of Geotechnical and Geoenvironmental Engineering,* 132(7), pp. 830-841.

Xie, Y., Leshchinsky, B. and Han, J. (2019). "Evaluation of bearing capacity on geosynthetic-reinforced soil structures considering multiple failure mechanisms." *Journal of Geotechnical and Geoenvironmental Engineering,* 145(9), p.04019040.

Xiao, C., Han, J., Zhang, Z. (2016). "Experimental study on performance of geosynthetic-reinforced soil model walls on rigid foundations subjected to static footing loading." *Geotextiles and geomembranes,* 44(1), pp. 81-94.

Zheng, Y., Fox, P.J., Shing, P.B. and McCartney, J.S. (2019). "Physical model tests of half-scale geosynthetic reinforced soil bridge abutments. I: Static loading." *Journal of Geotechnical and Geoenvironmental Engineering,* 145(11), p.04019094.